Acta Crystallographica Section F
Structural Biology and Crystallization Communications
ISSN 1744-3091

Purification, crystallization and preliminary X-ray analysis of the dissimilatory sulfite reductase from *Desulfovibrio vulgaris* Miyazaki F

Hideaki Ogata,[a] Yasuhito Shomura,[b] Aruna Goenka Agrawal,[a] Amrit Pal Kaur,[a] Wolfgang Gärtner,[a] Yoshiki Higuchi[b] and Wolfgang Lubitz[a]*

[a]Max-Planck-Institut für Bioanorganische Chemie, Stiftstrasse 34-36, D-45470 Mülheim an der Ruhr, Germany, and [b]Graduate School of Life Science, University of Hyogo, Koto 3-2-1, Ako-gun, Hyogo, 678-1297, Japan

Correspondence e-mail: lubitz@mpi-muelheim.mpg.de

Received 21 July 2010
Accepted 17 August 2010

Dissimilatory sulfite reductase (Dsr) plays an important role in sulfate respiration in many sulfate-reducing bacteria. Dsr from *Desulfovibrio vulgaris* Miyazaki F has been purified and crystallized at 277 K using the sitting-drop vapour-diffusion method with PEG 3350 and potassium thiocyanate as precipitants. A data set was collected to 3.7 Å resolution from a single crystal at 100 K using synchrotron radiation. The Dsr crystal belonged to space group $P4_12_12$, with unit-cell parameters $a = b = 163.26$, $c = 435.32$ Å. The crystal structure of Dsr was determined by the molecular-replacement method based on the three-dimensional structure of Dsr from *D. vulgaris* Hildenborough. The crystal contained three $\alpha_2\beta_2\gamma_2$ units per asymmetric unit, with a Matthews coefficient (V_M) of 2.35 Å^3 Da^{-1}; the solvent content was estimated to be 47.7%.

1. Introduction

Dissimilatory sulfite reductase (Dsr; formerly desulfoviridin; EC 1.8.99.3) plays a key role in sulfate metabolism in many sulfate-reducing bacteria. In these organisms, sulfate is used as the terminal electron acceptor and hydrogen sulfide is formed as the final product in a dissimilatory sulfate reduction (Odom & Peck, 1981). It is known that there are three major steps in sulfate reduction (for a review, see Fritz *et al.*, 2005). In the first step, sulfate is activated by ATP-sulfurylase to yield adenosine 5′-phosphosulfate (APS) and pyrophosphate. In the second step, adenylylsulfate reductase catalyzes the two-electron reduction of APS to AMP and sulfite. In the last step, Dsr catalyzes a six-electron reduction converting sulfite to sulfide.

Dsr has 2–4 sirohaem and 10–32 nonhaem irons per $\alpha_2\beta_2\gamma_n\delta_m$ unit, depending on the species (organism) and the purification procedure (Crane & Getzoff, 1996; Oliveira *et al.*, 2008). The Dsr from *Desulfovibrio vulgaris* Miyazaki F (MF) is an $\alpha_2\beta_2\gamma_2$ complex (DsrABC) composed of two $\alpha\beta$ units that contain two sirohaems and eight Fe–S clusters. The two γ subunits are tightly bound to the $\alpha\beta$ units. The heterodimeric $\alpha_2\beta_2$ unit (DsrAB) is considered to be the functional unit (Aketagawa *et al.*, 1985). The α, β and γ subunits have molecular weights of approximately 53, 42 and 8 kDa, respectively. The solution NMR structure of the γ subunit (DsrC) from *Pyrobaculum aerophilum* and the X-ray crystal structure of DsrC from the hyperthermophilic archaeon *Archaeoglobus fulgidus* have been reported (Cort *et al.*, 2001; Mander *et al.*, 2005). A major difference between the NMR structure and the crystal structure was observed in the C-terminal region. In the crystal structure the C-terminal region is well ordered, in contrast to the NMR structure, which showed this region as being disordered. Cort and coworkers suggested that the flexibility of the C-terminal region could be rigidified on the binding of DsrC to another protein (Cort *et al.*, 2001). The crystal structure of DsrAB from *A. fulgidus* has been reported by Schiffer *et al.* (2008), showing two sirohaems and eight Fe–S clusters in the $\alpha_2\beta_2$ complex. In addition, the crystal structure of DsrABC from the sulfate-reducing bacteria *D. vulgaris* Hildenborough has recently been reported (Oliveira *et al.*, 2008). The $\alpha_2\beta_2\gamma_2$ units contain two sirohaem Fe–S clusters, two sirohydrochlorin Fe–S clusters and four Fe–S

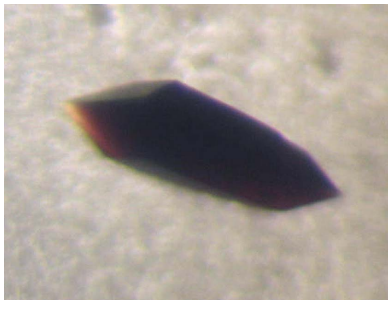

clusters. It was suggested that DsrC is involved in sulfite reduction, since DsrC can reach the sirohaem which is located between DsrA and DsrB.

In order to understand the mechanism of dissimilatory sulfate reduction, which plays a central role in the metabolism of sulfate-reducing bacteria, we purified DsrABC from the Gram-negative sulfate-reducing bacterium *D. vulgaris* MF. In this paper, we report the purification, crystallization and preliminary X-ray analysis of DsrABC from *D. vulgaris* MF.

2. Materials and methods

2.1. Sequence analysis

The protein was identified by N-terminal sequencing and MALDI–TOF mass spectrometry. The partial sequence was used to design degenerate primers for the α subunit of the Dsr of *D. vulgaris* MF in order to confirm the protein-based results (Kaur, 2009). Nucleotide sequencing was then completed from a cosmid clone of a genomic library of *D. vulgaris* MF (Kaur, 2009). The positive clone was identified by Southern hybridation of the cosmid DNA using a non-radioactive dioxygenin-labelled dUTP probe (Roche).

2.2. Protein purification

The protein was isolated from the cytosolic fraction of the sulfate-reducing bacterium *D. vulgaris* MF. Cell growth was carried out using the method described previously (Yagi *et al.*, 1968). Cells were lysed by sonication using a buffer containing 10 m*M* NaCl, 25 m*M* Tris–HCl pH 7.4, followed by centrifugation at 184 000*g* and 277 K for 90 min. All purification steps were performed at 277 K under aerobic conditions. The cytoplasmic fractions were collected and 0.25 n*M* Pefabloc SC (Biomol GmbH, Germany) was added as a serine protease inhibitor. The proteins were loaded onto a DEAE-Toyopearl 650S (Tosoh, Japan) anion-exchange column (linear gradient of 10–25% 1 *M* NaCl). The eluted DsrABC fractions from the DEAE column were concentrated to 5 ml and passed through a Sephacryl S200HR (GE Healthcare, Uppsala, Sweden) gel-filtration column. The collected fractions from this purification step were further purified using a Q-Sepharose (GE Healthcare, Uppsala, Sweden) strong anion-exchange column (linear gradient of 10–22.5% 1 *M* NaCl) and the eluted DsrABC fractions were again loaded onto a Q-Sepharose column (10–22.5% linear gradient of 1 *M* NaCl). For a final purification step, a HiLoad 26/60 Superdex 200 prep-grade gel-filtration column (GE Healthcare, Uppsala, Sweden) in 25 m*M* Tris–HCl buffer pH 7.4 was used. The quality of the samples was controlled by SDS–PAGE.

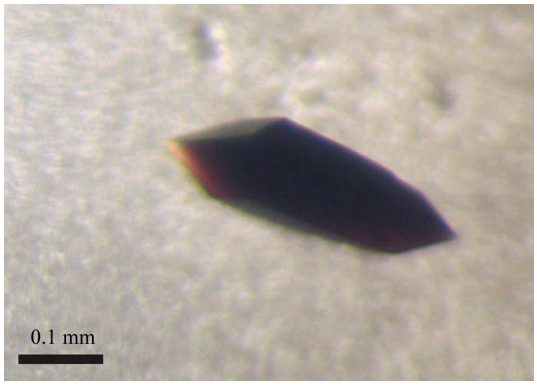

Figure 1
Single crystal of DsrABC from *D. vulgaris* MF.

Table 1
Data-collection statistics.

Values in parentheses are for the highest resolution shell.

Wavelength (Å)	0.91840
Space group	$P4_12_12$
Unit-cell parameters (Å)	$a = b = 163.26$, $c = 435.32$
Resolution (Å)	34.1–3.7 (3.8–3.7)
No. of observed reflections	500302
No. of unique reflections	61240
$R_{\rm merge}$†	0.134 (0.486)
Completeness (%)	96.0 (92.2)
$\langle I/\sigma(I)\rangle$	16.5 (5.2)

† $R_{\rm merge} = \sum_{hkl}\sum_i |I_i(hkl) - \langle I(hkl)\rangle| / \sum_{hkl}\sum_i I_i(hkl)$, where $I_i(hkl)$ is the intensity of the ith observation and $\langle I(hkl)\rangle$ is the mean intensity of the reflections.

2.3. Crystallization

The purified protein was concentrated to 20 mg ml^{-1} in 10 m*M* HEPES, pH 7.4 and 10 m*M* KCl by centrifugation using an Amicon Ultra Centrifugal filter device (30 kDa molecular-weight cutoff; Millipore). Crystallization screening was carried out at 277 K by the sitting-drop vapour-diffusion method. Crystal Screen Cryo, Crystal Screen 2, PEG/Ion, PEG/Ion 2, Natrix and MembFac (Hampton Research, California, USA) and Wizard I, Wizard II, Cryo I and Cryo II (Emerald BioSystems, Washington, USA) were used for initial screening. Protein droplets were prepared by mixing 10 µl DsrABC solution and 10 µl reservoir buffer solution and were set up in a Cryschem plate (Hampton Research) with 1 ml reservoir solution. After three weeks, crystals were obtained. Crystals suitable for diffraction experiments were obtained using 25%(*w*/*v*) PEG 3350, 0.2 *M* KSCN with 10 m*M* KCl, 10 m*M* HEPES, pH 7.4 buffer (Fig. 1). The crystal dimensions were typically 0.3 × 0.3 × 0.1 mm (Fig. 1).

2.4. Data collection and analysis

In order to collect data at cryogenic temperature, a crystal was separated, dipped into cryoprotectant [15% glycerol, 25%(*w*/*v*) PEG 3350, 0.2 *M* KSCN] and subsequently frozen in a stream of nitrogen gas at 100 K. Optimization of the cryoconditions was carried out using BL41XU at SPring-8 (Hyogo, Japan) and PXIII at SLS (Villigen, Switzerland). A complete native data set was collected to 3.7 Å resolution. Diffraction data collection was carried out at 100 K on beamline BL14.2 at BESSY II (Berlin, Germany). For the native data set, 500 images of 7 s exposure time and 0.2° oscillation were collected using a Rayonix 225 detector. The crystal-to-detector distance was maintained at 350 mm. The diffraction images were indexed and integrated using the program *XDS* (Kabsch, 2010). Scaling was carried out with *XSCALE* (Kabsch, 2010).

3. Results

The protein sequence of DsrABC from *D. vulgaris* MF was deduced by translating the operon sequenced from a cosmid library and was confirmed by partial N-terminal sequencing. DsrABC was successfully purified and crystallized. Single crystals were obtained at 277 K using the sitting-drop vapour-diffusion method with PEG 3350 and KSCN as precipitating agents. The crystals diffracted to 3.7 Å resolution and belonged to space group $P4_12_12$, with unit-cell parameters $a = b = 163.26$, $c = 435.32$ Å. The data-collection conditions and the results obtained are summarized in Table 1. It was assumed that the crystal contained two or three $\alpha_2\beta_2\gamma_2$ units per asymmetric unit, with

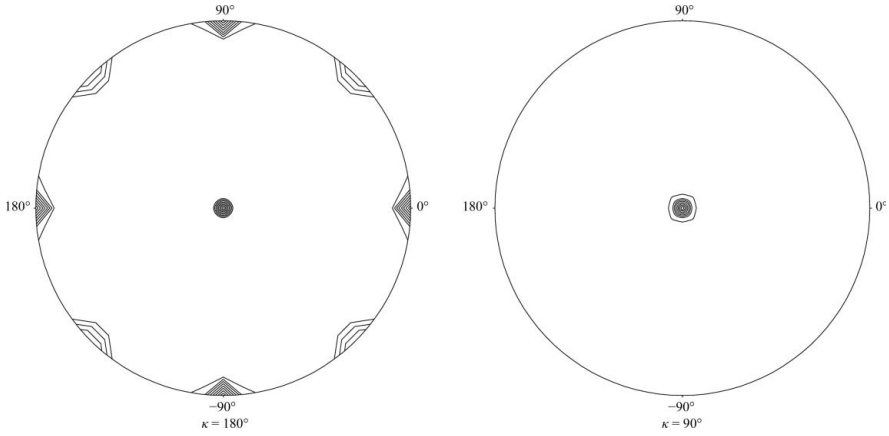

Figure 2
Self-rotation function ($\kappa = 180°$ and 90° sections) calculated with the data scaled in space group $P4_12_12$. Data in the resolution range 20–3.7 Å and an integration radius of 100 Å were used.

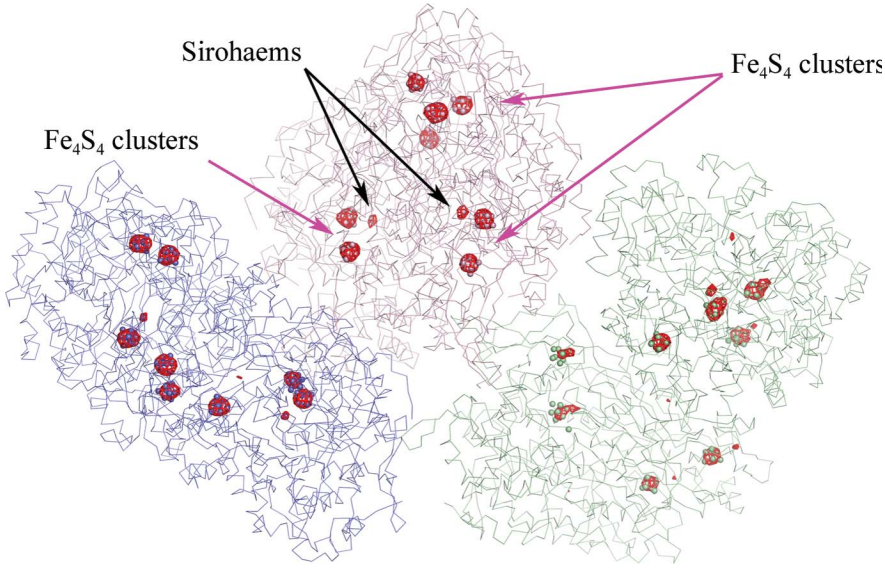

Figure 3
The $F_{obs} - F_{calc}$ difference Fourier map (4σ cutoff) of the three $\alpha_2\beta_2\gamma_2$ units in the asymmetric unit. The three $\alpha_2\beta_2\gamma_2$ units are depicted in blue, purple and green. The Fe–S clusters and the irons of the sirohaem are represented as spheres.

a Matthews coefficient (V_M) of 3.52 or 2.35 Å^3 Da^{-1} and a solvent content of 65.1 or 47.7%, respectively. The self-rotation function calculated using the program *POLARRFN* (Collaborative Computational Project, Number 4, 1994) did not show the presence of noncrystallographic symmetry (Fig. 2). The molecular-replacement method was applied using the program *MOLREP* (Vagin & Isupov, 2001) from the *CCP*4 program suite. The data for DsrABC from *D. vulgaris* Hildenborough (PDB entry 2v4j; Oliveira *et al.*, 2008) were used as coordinates for the search model. After calculation of the electron-density map using the molecular-replacement solution and rigid-body refinement with the program *REFMAC*5 (Vagin *et al.*, 2004), three $\alpha_2\beta_2\gamma_2$ units were identified in the asymmetric unit. The structure was refined to R and R_{free} values of 33.2% and 33.4%, respectively. In the $F_{obs} - F_{calc}$ difference Fourier map calculated without the metal centres, strong peaks indicated the presence of the Fe–S clusters and sirohaems (Fig. 3). A Matthews coefficient (V_M) of 2.35 Å^3 Da^{-1} was found and the solvent content was estimated to be 47.7%. In the electron-density map, the C-terminal region of the γ subunit was confirmed to bind between the α subunit (DsrA) and the β subunit (DsrB).

We thank Patricia Malkowski and Birgit Nöring for their help during sample preparation. Koji Nishikawa is gratefully acknowledged for helpful discussions. We thank the staff of beamlines BL41XU and BL38B1 at SPring-8 (Hyogo, Japan), beamline BL14.2 at BESSY II (Berlin, Germany) and the PXIII beamline at SLS (Villigen, Switzerland) for their assistance during data collection. This work was supported by the Max Planck Society.

References

Aketagawa, J., Kojo, K. & Ishimoto, M. (1985). *Agric. Biol. Chem.* **49**, 2359–2365.
Collaborative Computational Project, Number 4 (1994). *Acta Cryst.* D**50**, 760–763.
Cort, J. R., Mariappan, S. V. S., Kim, C.-Y., Park, M. S., Peat, T. S., Wald, G. S., Terwilliger, T. C. & Kennedy, M. A. (2001). *Eur. J. Biochem.* **268**, 5842–5850.
Crane, B. R. & Getzoff, E. D. (1996). *Curr. Opin. Struct. Biol.* **6**, 744–756.
Fritz, G., Einsle, O., Rudolf, M., Schiffer, A. & Kroneck, P. M. H. (2005). *J. Mol. Microbiol. Biotechnol.* **10**, 223–233.
Kabsch, W. (2010). *Acta Cryst.* D**66**, 125–132.
Kaur, A. P. (2009). Dissertation. Heinrich-Heine-Universität Düsseldorf, Germany.
Mander, G. J., Weiss, M. S., Hedderich, R., Kahnt, J., Ermler, U. & Warkentin, E. (2005). *FEBS Lett.* **579**, 4600–4604.
Odom, J. M. & Peck, H. D. (1981). *J. Bacteriol.* **147**, 161–169.
Oliveira, T. F., Vonrhein, C., Matias, P. M., Venceslau, S. S., Pereira, I. A. C. & Archer, M. (2008). *J. Biol. Chem* **283**, 34141–34149.
Schiffer, A., Parey, K., Warkentin, E., Diederichs, K., Huber, H., Stetter, K. O., Kroneck, P. M. H. & Ermler, U. (2008). *J. Mol. Biol.* **379**, 1063–1074.
Vagin, A. A. & Isupov, M. N. (2001). *Acta Cryst.* D**57**, 1451–1456.
Vagin, A. A., Steiner, R. A., Lebedev, A. A., Potterton, L., McNicholas, S., Long, F. & Murshudov, G. N. (2004). *Acta Cryst.* D**60**, 2184–2195.
Yagi, T., Honya, M. & Tamiya, N. (1968). *Biochim. Biophys. Acta*, **153**, 699–705.